

Asadi

No code

Gravitational millilensing as a probe of dark matter on subgalactic scales

Abstract

The mismatch between the faint-end of galaxy luminosity function and the low-mass end of the dark matter halo mass function has been around for over a decade now. This is a largely-untested challenge for the cold dark matter model. While gravitational lensing provides a unique method to detect the predicted extremely faint or completely dark galactic subhalos, observations of very high angular resolution are required. Previous VLBA maps of the gravitationally-lensed quasar in B1152+199 have resulted in a tentative detection of such a substructure with mass $1e5-1e7$ Msolar, based on the jet bending seen in one of the two macroimages in this system. Here, we propose 3.6 cm observations of B1152+199, using the global VLBI array, providing ~ 4 times better resolution (0.7 mas) than the 6 cm VLBA data to A) confirm the jet bending and B) search for previously unresolved distortions in the curved jet to provide the first robust detection of gravitational millilensing by dark halo substructure.

Applicants

Name	Affiliation	Email	Country	Potential observer
Saghar Asadi	Stockholm University (Department of Astronomy)	saghar.asadi@astro.su.se	Sweden	Pi
Dr Erik Zackrisson	Stockholm University (Department of Astronomy)	ez@astro.su.se	Sweden	
Prof John Conway	Onsala Space Observatory, Chalmers University	john.conway@chalmers.se	Sweden	
Eskil Varenius	Chalmers University of Technology	eskil.varenius@chalmers.se	Sweden	
Dr Emily Freeland	Stockholm University	emily.freeland@astro.su.se	Sweden	
Dr. Kaj Wiik	University of Turku (Tuorla Observatory)	kaj.wiik@utu.fi	Finland	
DR. JUAN GONZALEZ	STOCKHOLM UNIVERSITY (Oskar Klein Centre)	juan.gonzalez@astro.su.se	SWEDEN	
Hannes Jensen	Stockholm university (Department of Astronomy)	hjens@astro.su.se	Sweden	

Contact Author

Title		Institute	Stockholm University
Name	Saghar Asadi	Department	Department of Astronomy
Email	saghar.asadi@astro.su.se	Address	Stockholm University AlbaNova University Center Department of Astronomy
Phone(first)	+46 8 5537 8533	Zipcode	106 91
Phone(second)		City	Stockholm
Fax		State	
		Country	Sweden

Summary of Observations

Observation number	Number of targets	Network	Hours requested	Waveband	Number of epochs	Aggregate bitrate	Correlator	e-EVN
1	1	EVN, EVN with individual limitations, VLBA	12.0, 12.0, 12.0	3.6 cm	1	1024	JIVE	No

*Scientific Category: Extragalactic**Scheduling Assistance Required: Consultation**Rapid Response Science: Not specified**Students involved*

Student	Level	Applicant	Supervisor	Applicant	Expected completion date	Data required
Saghar Asadi	Doctor	Yes	Dr Erik Zackrisson	Yes	2016/07	Yes
Hannes Jensen	Doctor	Yes	Prof Garrelt Mellema	No	2014/08	No
Eskil Varenius	Doctor	Yes	Prof John Conway	Yes	2016/09	No

*Linked proposal submitted to this TAC: No**Linked proposal submitted to other TACs: No**Relevant previous Allocations: Yes*

Experiment EZ024

PI. Zackrisson

No additional remarks

1 Gravitational millilensing as a probe of dark halo substructure

In the current model of cosmic structure formation, massive halos in the local Universe have grown over time by accreting mass from smaller halos in their vicinity during a period of several billion years. However, some of these low-mass halos temporarily survive in the form of subclumps within the massive halo they fell into. The cold dark matter (CDM) model has been very successful in explaining the large-scale structure of the Universe through such hierarchical assembly. However, it is yet to be confirmed on sub-galactic scales. A generic prediction of the theory is that dwarf galaxies should form within the dark matter subhalos residing in the halos of Milky Way-sized galaxies. This prediction results in a substantial discrepancy between the number of expected dark subhalos and the number of observed dwarf galaxies in the local Universe. About 10% of the total mass of a galaxy-sized halo at $z = 0$ should be in the form of bound substructures (Gao et al. 2011), greatly outnumbering the observed satellite galaxies around the Milky Way and Andromeda (Klypin et al. 1999, Moore et al. 1999). Therefore, confirmation of the Λ CDM scenario on this scale requires the existence of large numbers of low-mass dark subhalos, in which star formation has been quenched (Maccò et al. 2010).

Gravitational lensing provides an independent test for the existence of such very faint or completely dark substructures. One can make use of strongly lensed sources at intermediate redshifts ($z \sim 1-2$) to probe the foreground lens galaxy for dark subhalos (Figure 1). This method looks for small-scale surface brightness perturbations in a lensed image which are not replicated in others, and therefore requires high-resolution observations of source images.

Using optical/near-IR imaging (resolution ~ 100 mas) of Einstein rings with the Hubble Space Telescope and Keck, Vegetti et al. (2010, 2012) were able to detect two dark substructures of mass $10^8-10^9 M_\odot$. Curiously, these observations seem to indicate a subhalo mass fraction that is significantly higher than predicted by standard CDM, and possibly also a flatter subhalo mass function slope (Vegetti et al. 2012). Alternatively, there may be other types of dark matter overdensities present within these systems, like primordial black holes or ultracompact minihalos (e.g. Zackrisson et al. 2013).

By using VLBI to map images of macrolensed radio jets with milliarcsecond or sub-milliarcsecond resolution, dark substructures with masses several orders of magnitude below the HST/Keck detection limits can in principle be probed (e.g. Wambsganss & Paczynski 1992, Metcalf & Madau 2001, Zackrisson et al. 2013). Gravitational lensing at this angular scale is commonly referred to as millilensing. However, due to the much smaller linear sizes of typical radio jets ($\sim 1-10$ pc at the relevant frequencies) compared to the typical source sizes at optical/near-IR wavelengths (~ 1 kpc), the probability of detecting subhalos in a randomly chosen macrolensed system is much smaller than when optical/near-IR macrolenses are used as targets (Zackrisson et al. 2013). Consequently, no clear-cut detections of gravitational millilensing have so far been made.

B1152+199 is a strong lensing system, discovered as part of the Cosmic Lens All-Sky Survey (CLASS), consisting of a quasar's radio jet at $z = 1.019$ lensed by a single galaxy at $z = 0.439$ into two images which are $1.56''$ apart in the sky (Myers et al. 1999). The single-lens model of the system, based on 5 GHz VLBA maps of the blazar as well as I - and V -band HST images revealing the lens galaxy (Rusin et al. 2002), was shown to be insufficient to explain the anomalous curvature in one of the images which is absent in the other image (Figure 3). Metcalf (2002), therefore, suggested that the bending in image B is not an intrinsic feature of the source, but rather due to one (or more) perturber(s) of $M \sim 10^5-10^7 h^{-1} M_\odot$ on the lens plane and along the line of sight of image B. Reproducing the observed feature required lenses with more centrally concentrated mass profiles than CDM subhalos. However, the resolution of the data at 5 GHz (~ 3 mas where image B is only ~ 15 mas along) barely allows further constraints on the mass and inner structure of the perturber(s).

The preliminary analysis of a new 5 GHz data set using the European VLBI Network (Experiment *EJ010* – PI. *Jackson*) indicates a persisting curvature in image B (Figure 4). Therefore, given the 10-year time difference between the two data sets and the fact that morphological anoma-

lies produced by millilensing of halo substructures in the $\geq 10^4 M_\odot$ mass range remain stationary over hundreds to thousands of years, the (milli)lensing nature of the jet curvature seems to be confirmed.

Our group also made an attempt to observe the same target at 22 GHz with the EVN, which would potentially give an angular resolution of ≈ 0.3 mas (Experiment *EZ024* – PI. *Zackrisson*). However, after reducing the data, it was clear that due to lack of proper data from the longest baselines in the array (responsible for smallest angular scales on the map), and the very small intrinsic jet size at such a high frequency, image A (the more extended image) is barely resolved in 22 GHz maps. Therefore, further attempt to resolve or perform any lens modeling on image B would be futile at this frequency. However, even though the data were not good enough to properly analyse the shape of the lensed images, we could improve our astrometry of the images.

2 Proposed observations and technical details

The goal of the proposed project is to map the B1152+199 system at 8.3 GHz with 0.7 mas resolution to **A**) confirm the jet bending seen in two epochs of 5 GHz data and **B**) search for previously unresolved distortions. Since we require the highest resolution and best imaging fidelity, we request the full EVN+VLBA array available at 3.6 cm: Wb, Eb, Mc, Nt, On-60, Sh, Ur, Ys, Wz, Hh, Sv, Zc, Bd + VLBA. We request 12 hours of observation time from 04 to 16 GST.

We estimate that correlating in the middle of the two lensed images (1.56" apart) using 1 MHz channel width and 1 second integration time would result in up to 4.76% coherence loss *for the longest baselines* at the position of the lensed images, due to smearing. We find this acceptable and therefore request one single correlation center between the two images.

We will observe with a cycle of 3 min on target (between the two lensed images) and 1 min on the calibrator J1157+1638 (3.06° away from the target) which has VLBA 8.3 GHz correlated flux density of 200 mJy on the longest baselines. It will be used for phase-referencing to derive delay, rate and phase corrections which will be transferred to the target visibilities. The expected RMS noise on the baseline Hh-Eb using 1 minute integration and one 16 MHz subband is 4 mJy, i.e. an SNR of 50 for this calibrator. We also plan to observe the bright (0.8 Jy on longest baselines) and very compact calibrator J1159+2914 (9.6° from target) a few times during the experiment as fringe finder to help correcting for the major delay and rate offsets in the correlation process.

The spectrum of the source is flat up to 15 GHz and beyond (Figure 2) and Rusin et al. (2002) present 5 GHz VLBA images with core flux densities of 33 mJy and 12 mJy respectively. We expect of order 30 mJy of correlated flux density from the brightest image at 8.3 GHz.

Assuming 20% of the requested 12h is lost to slewing and fringe finder scans, we expect 432 min total integration time on target. Assuming 1024 Mbps, 2 bit sampling, dual polarisation, 8 subbands and 16 MHz/subband we estimate the theoretical RMS image noise to be $5.1 \mu\text{Jy/beam}$ using natural weighting¹. This assumes good weather and all telescopes observing all the time. Even if, given other weighting and non-optimum weather etc., the final map noise is as high as $51 \mu\text{Jy/beam}$, imaging with dynamic range of 200-650:1 is possible.

References

- Gao et al. 2011, MNRAS, 410, 2309 ★ Klypin et al. 1999, ApJ, 522, 82 ★ Macciò et al. 2010, MNRAS, 402, 1995 ★ Metcalf, R. B., & Madau, P. 2001, ApJ, 563, 9 ★ Metcalf, R. B. 2002, ApJ, 580, 696 ★ Moore et al. 1999, ApJ 524, L19 ★ Myers et al. 1999, ApJ 117, 2565 ★ Rusin, D., et al. 2002, MNRAS, 330, 205 ★ Vegetti et al. 2010, MNRAS, 408, 1969 ★ Vegetti et al. 2012, Nature, 481, 341 ★ Wambsganss, J. & Paczynski, B. 1992, ApJ, 397, L1 ★ Zackrisson E. & Riehm T. 2010, Advances in Astronomy, vol. 2010, 1 ★ Zackrisson et al. 2013, MNRAS, 431, 2172

¹<http://www.evlbi.org/cgi-bin/EVNcalc>

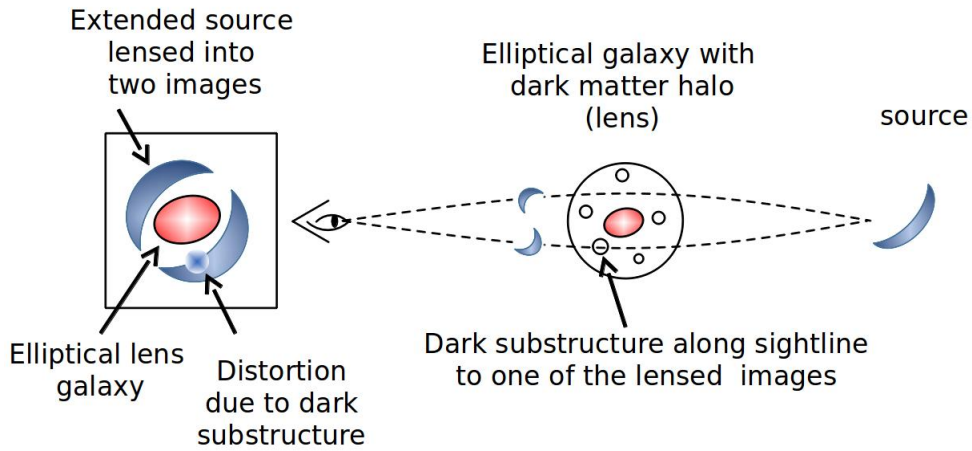


Figure 1: Schematic illustration of gravitational millilensing as a probe of dark halo substructure. A foreground galaxy with a dark matter halo produces two macroimages of a background light source. A subhalo (or other substructure) located in the dark halo intercepts the path of one of these macroimages and produces a small-scale distortion (millilensing) in its surface brightness distribution. Whereas morphological anomalies intrinsic to the source should be mimicked in both macroimages, millilensing will affect each macroimage differently, and typically turn up just in one image.

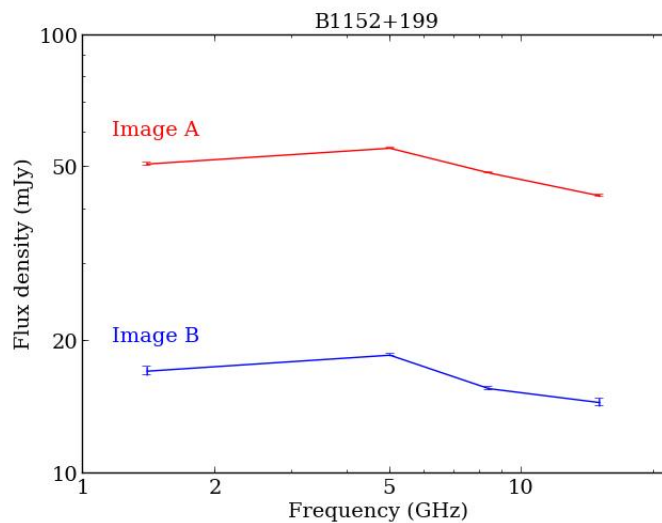


Figure 2: While the intrinsic size of the jet decreases at higher frequencies –where higher angular resolution can be achieved– the exact size of the source at any arbitrary frequency is not easily known. However, given the resolved 5 GHz maps and flux density measurements of the unresolved source (i.e. core + jet) at various frequencies including the 8.3 GHz by Myers et al. (1999), jet length could be estimated based on the synchrotron lifetime of electrons. The ≈ 0.8 times larger flux density of each image at 5 GHz with respect to that at 8.3 GHz, suggests only a ≈ 0.2 times decrease in jet length when going from the former frequency to the latter, while the expected angular resolution at 8.3 GHz (0.7 mas) is ≈ 4 times better than that at 5 GHz. Therefore, the 8.3 GHz map would allow tighter constraints on the mass and density profile of the lens perturber in the system.

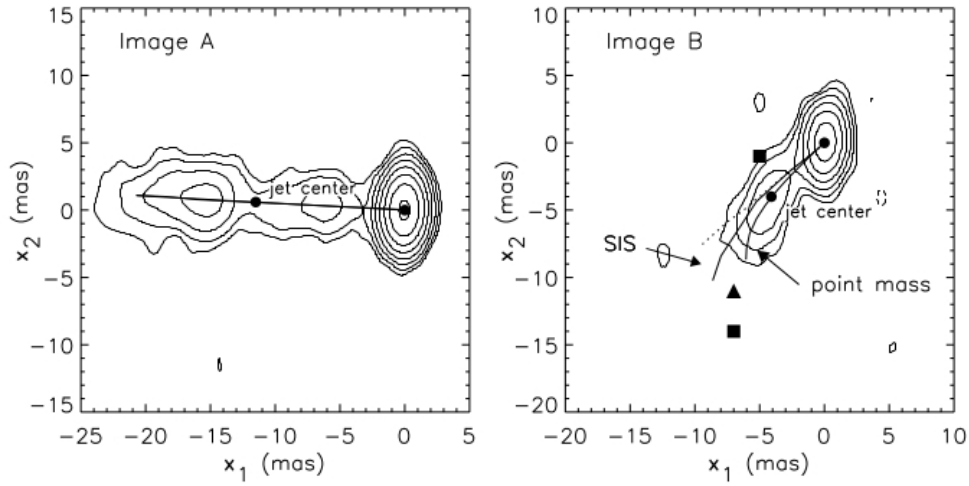


Figure 3: The VLBA 5-GHz maps (Rusin et al. 2002; beam $3.6 \times 1.9 \text{ mas}^2$) of the two macroimages of B1152+199, overlaid with lens models from Metcalf (2002). The slight curvature of the jet in the right panel (image B) is attributed to millilensing by a substructure located close to this macroimage. In the absence of such substructure, the jet in the right macroimage would follow the path given by the dotted, straight line (a poor fit to the data). The two curved paths are produced when different forms of substructures are introduced. The lowermost curve is given by a point-mass substructure (IMBH) of mass $\sim 10^5\text{--}10^7 M_\odot$ located at the position of the triangle. The intermediate curve is reproduced by two SIS substructures (squares) with slightly higher, but poorly constrained masses. Singular isothermal spheres (SIS) are proper models for galaxy-sized halos, centrally dominated by baryons. The central slope is, however, too steep compared to dark subhalos. Metcalf (2002) emphasizes that while the jet bending indicates some form of millilensing, the substructure solution (in terms of substructure position and mass) to these data is by no means unique. The proposed high-resolution observations could considerably alter the situation.

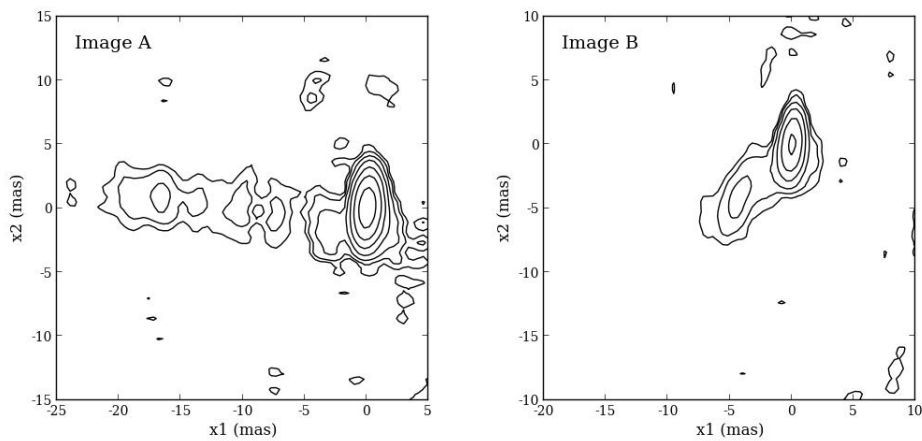


Figure 4: The archival EVN 5-GHz maps (beam $3.8 \times 1.4 \text{ mas}^2$) of the two macroimages of B1152+199 (Experiment *EJ010* – PI. *Jackson*). Contour levels are the same as in figure 2; the lowest contour is 3 times the map rms noise in figure 2 ($75 \mu \text{ Jy beam}^{-1}$) and each contour level increases by a factor of 2. The slight curvature of the jet in the right panel (image B) seems to be unchanged over 10 years. This, in addition to the much shorter ($\approx 40\text{--}70$ days) gravitational time delay of the system, suggests that the curvature cannot be due to jet precession.

Observation details of observation 1

e-EVN observation?							
No							
Waveband requested							
3.6 cm							
Global Network standard bands							
Requested telescopes, times per network							
Network	Requested telescopes					Hours	GST Range
EVN	Wb, Ef, Mc, Nt, On-60, Sh, Ur, Ys, Sv, Zc, Bd					12.0	04-16
EVN with individual limitations	Hh, Wz					12.0	04-16
VLBA	Br, Fd, Hn, Kp, La, Mk, Nl, Ov, Pt, Sc					12.0	04-16
No Preferred VLBI session or range of dates for scheduling							
No Dates which are NOT acceptable							
Recording format specification (network defaults)							
Number of polarizations :		2		Number of bits per sample:		2	
Number of subbands per polarization :		8		Number of basebands :		16	
Bandwidth per subband :		16 MHz		Number of Msamples per second per subband:		32	
Oversampling :		1		Aggregate bitrate :		1024 Mbps	
Special issues: no							
Multi-epoch observation							
No Multi-epoch observation							
Processor Information							
Process or	Special Processing	Averaging time		Spectral channels per Baseband channel	Max. antennas	Independent correlator passes	
JIVE	no	1		16	23	1	
Target Sources							
Field	RA	Dec	Equinox	Total flux density (Jy)	Correlated flux density (mJy)	Peak/RMS	Field of View (arcsec)
B1152+199	11:55:18.328885	+19:39:41.60530	J2000	0.05	30.0	200.0	2.0
Phase Reference Sources							
Field	RA	Dec	Equinox	RA Error (mas)	Dec Error (mas)	Corr. Flux (mJy)	Separation from target (deg)
J1157+1638	11:57:34.836267	+16:38:59.65005	J2000	0.34	0.27	200.0	3.06
J1159+2914	11:59:31.833911	+29:14:43.82687	J2000	0.23	0.4	800.0	9.6